Hydrogen absorption in oxide-supported palladium nanocrystals

M. Wilde,[1,2,*] K. Fukutani,[1,2] M. Naschitzki,[3] and H.-J. Freund[3]
[1]*Institute of Industrial Science, University of Tokyo, Komaba, Meguro-ku, 153-8505 Tokyo, Japan*
[2]*CREST-JST, Komaba, Meguro-ku, 153-8505 Tokyo, Japan*
[3]*Fritz-Haber-Institut der Max-Planck-Gesellschaft, Faradayweg 4-6, D-14195 Berlin, Germany*
(Received 25 February 2008; published 31 March 2008)

Substantial hydrogen absorption in nanometer-sized palladium crystallites on a thin film alumina support is observed at 90–350 K under low H_2 pressure conditions ($<2\times10^{-3}$ Pa) by $^1H(^{15}N,\alpha\gamma)^{12}C$ nuclear reaction analysis. The enthalpy of H solution varies with the absorbed H content and with $-(0.28\pm0.02)$ eV/H exceeds that of bulk Pd at H/Pd ratios below 0.20. By resolving absorbed H from surface-adsorbed H, this enhanced H stability is identified as an intrinsic volume property of the small crystallites rather than being associated with particular binding sites on or near their surfaces.

DOI: 10.1103/PhysRevB.77.113412 PACS number(s): 68.47.Jn, 61.46.−w, 64.70.Nd, 82.33.Fg

Hydrogen absorption by finely dispersed palladium is relevant for metal hydride H storage and heterogeneous catalysis. Oxide-supported Pd particles catalyze hydrogenation reactions of olefins.[1] Model catalysts of nanometer-sized Pd crystallites deposited in ultrahigh vacuum (UHV) on the thin alumina film on NiAl(110) (Ref. 2) exhibit increased reactivity for ethene hydrogenation compared to Pd(111) single crystals.[3,4] This was attributed to hydrogen absorbed by the Pd clusters. Their extensive characterization by surface analytical techniques[2] even includes atomic resolution imaging of individual cluster facets with scanning tunneling microscopy (STM).[5] Yet, the only evidence for absorbed hydrogen stems from temperature programmed desorption (TPD) spectroscopy.[3,4] This leaves the distinction of absorbed H from H bound to the inherently large number of corners, edges, and surface defects of the small clusters a controversial issue. A straightforward proof for H absorption by the Pd nanocrystals in low H_2 pressure environments is required to judge the possible involvement of absorbed H in catalysis. In terms of H absorption, Pd nanoparticles further differ from bulk Pd by an increased H solubility in the dilute α-phase and a narrowed α/β two-phase coexistence region.[6,7] Abundant subsurface sites in the nanoparticles, available due to their large surface-to-volume ratio, were suggested to explain these properties.

In this Brief Report, we describe the unambiguous distinction of surface-adsorbed and volume-absorbed hydrogen on or in Pd nanocrystals on Al_2O_3/NiAl(110) with nuclear reaction analysis (NRA),[8] as previously applied to Pd(100) single crystals.[9] Here, we match the increased NRA depth resolution in grazing ^{15}N ion incidence[10,11] to the Pd cluster size in order to selectively monitor the H content in the crystallites while excluding surface H from detection. It is thus clarified that the volume of the small crystallites rather than their surface (including first-layer subsurface sites) provides enhanced H solubility compared to bulk Pd in the dilute regime of H/Pd<0.20. This suggests that nanoparticles owe their increased H solubility to their free boundary surfaces; unlike agglomerated grains in macroscopic bulk material, they experience no spatial confinement of their lattice expansion upon H absorption.

The 5 MV tandem accelerator at the Research Center for Nuclear Science and Technology (University of Tokyo) delivered an energy-monochromatized ($\Delta E=3$ keV) $^{15}N^{2+}$ ion beam of 10–20 nA for the NRA measurements. The 4.43 MeV γ rays emitted in the $^1H(^{15}N,\alpha\gamma)^{12}C$ nuclear reaction at the narrow 6.385 MeV energy resonance (E_{res}) are detected with a $Bi_4Ge_3O_{12}$ scintillator, providing the signal proportional to the H content in the target after normalization by the incident ^{15}N ion charge. H depth profiles are obtained by recording the γ yield as a function of the ^{15}N ion energy (E_i). E_i and the stopping power (dE/dz) (3.90 keV/nm for Pd)[12] define the probing depth (z) as

$$z=\frac{E_i-E_{res}}{(dE/dz)\cos(\alpha_i)}, \tag{1}$$

i.e., surface H ($z=0$) is detected at $E_i=E_{res}$ and absorbed H at $E_i>E_{res}$. A 3.86-fold increased depth resolution is realized at an ion incidence angle α_i of 75° relative to surface-normal incidence ($\alpha_i=0°$). The well-ordered thin alumina film was grown on a cleaned NiAl(110) crystal by *in situ* oxidation.[13] Pd (99.95%, Goodfellow) was deposited at 300 K at a calibrated rate of 0.34 Å/min from an electron beam evaporator (Omicron EFM-3), while a bias voltage applied to the sample protected the oxide from sputtering with Pd ions. A Pd coverage of 5.85 Å was chosen to yield the maximum density of well-faceted Pd crystallites ($\sim7.5\times10^{11}$ cm^{-2}).[5] At this coverage, the Pd clusters have a narrow size distribution of ~2 nm average height, a height to width aspect ratio of 0.18 ± 0.03, and are nearly uniformly dispersed with only minor preference of steps and domain boundary defects of the oxide support.[2,5] The Pd crystallites have well-ordered triangular or hexagonal shapes with flatted (111) terrace tops, exposing ~90% (111) and ~10% (100) facets.[2,5] As confirmed by NRA, neither H_2 nor atomic H adsorbs on the bare Al_2O_3 substrate at $T>90$ K, ensuring that the NRA signal entirely originates from Pd-bound H. During the NRA measurements, the UHV chamber (base pressure of 7×10^{-9} Pa) was filled with ultrapure H_2 from a PdAg purifier up to 2×10^{-3} Pa limited by the gas load into the accelerator. Consecutive depth profile scans verified that the ion beam does not alter the Pd cluster morphology [Fig. 1(a)]. Repeated

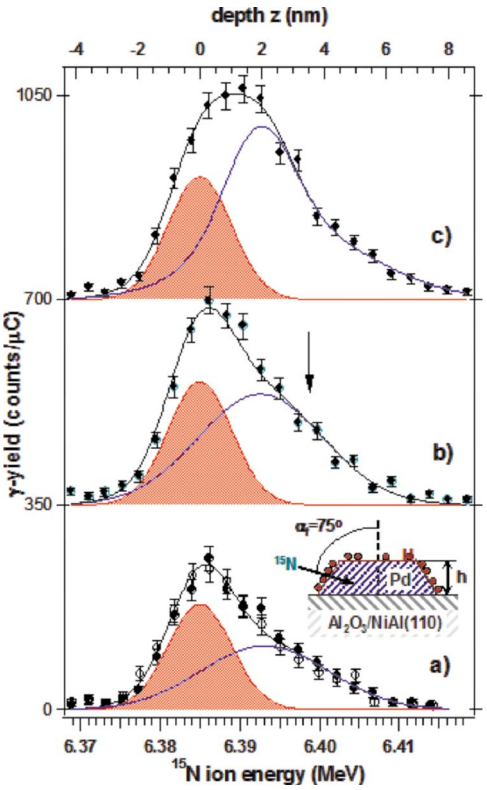

FIG. 1. (Color online) NRA yield curves of 5.85 Å $Pd/Al_2O_3/NiAl(110)$ at 90 K for H_2 pressures of (a) 2×10^{-5} Pa, (b) 6×10^{-4} Pa, and (c) 2×10^{-3} Pa. Profile (a) consists of two consecutive scans (filled and open circles) demonstrating the reproducibility of the measurement. Inset: grazing ion incidence geometry and schematic Pd cluster morphology.

cluster preparations by depositing the same Pd amount lead to reproducible H depth profiles.

NRA yield curves of the 5.85 Å $Pd/Al_2O_3/NiAl(110)$ cluster system at 90 K are shown in Fig. 1 for a range of H_2 pressures. The NRA signature of surface H on Pd is an ~10 keV wide [full width at half maximum (FWHM)] Gaussian form centered at E_{res} due to a zero-point vibrational Doppler effect.[9,14] Compared to this, all yield curves are asymmetrically broadened on the high energy side, indicating that H is not only adsorbed on the Pd cluster surface but also absorbed in their interior. With increasing H_2 pressure, the profile height saturates at ^{15}N energies near E_{res} between 2×10^{-5} and 6×10^{-4} Pa, whereas the intensity in the tailing grows further as the H_2 pressure is raised to 2×10^{-3} Pa. This implies that the H coverage on the crystallite surface saturates below 6×10^{-4} Pa H_2, while vacant H absorption sites still remain inside the clusters that fill at higher H_2 pressures. Surface saturation before the volume is natural as the H adsorption energy on metals (~−0.5 eV/H for H/Pd) (Refs. 15 and 16) is generally higher than the enthalpy of solution[17] (ΔH_s=−0.1 eV/H in Pd).[18] We determine the relative quantities of surface-adsorbed and volume-absorbed H by decomposing the yield curves (a) and (b) into the sum of two Gaussian forms (solid lines in Fig. 1), where FWHM and center of the surface H component are fixed to 10 keV and 6.385 MeV, respectively. The yield curve of absorbed H is additionally convolved with energy straggling of ^{15}N in Pd, the size and approximately random spatial distribution of the Pd particles on the oxide support, their morphology projection in the ion incidence direction, and a possibly inhomogeneous H depth distribution inside the clusters. Extracting such information from the yield curves is not straightforward, as will be discussed later. The second Gaussian form only serves to determine the mean H depth and the absorbed H quantity to evaluate the H_2 pressure-dependent H/Pd composition. Since the H coverage on low-index Pd surfaces exposed by the crystallites saturates at 10^{15} cm^{-2} (1 ML),[9,15,16] the integrated surface H component in the profile at 6×10^{-4} Pa [Fig. 1(b)] represents an intrinsic calibration standard for this layer density to which the intensity of absorbed H can be directly compared because its shallow depth distribution range is of the same order as the surface peak width. The H/Pd composition then follows from the intensity ratio of absorbed to surface H and the amount of deposited Pd (5.85 Å). A saturated surface H peak is subtracted from the wider profile at 2×10^{-3} Pa H_2 [Fig. 1(c)], and the absorbed H quantity is obtained by integrating the residual. The H/Pd ratio is found to continuously increase and is proportional to $p(H_2)^{1/2}$ from 0.35 ± 0.04 at 2×10^{-5} Pa to 0.80 ± 0.08 at 2×10^{-3} Pa H_2, indicating dissociative H absorption and significant hydrogenation of the clusters. From the proportionality constant, a rough estimate for the enthalpy of H solution in this high H concentration range is obtained as $\Delta H_s=(-0.12\pm0.11)$ eV/H, which reasonably compares to the value of bulk Pd.[18] Large H contents (H/Pd=0.8) in the same $Pd/Al_2O_3/NiAl(110)$ cluster system were also inferred from TPD measurements.[19] The present NRA study confirms that substantial H absorption by the Pd clusters occurs even under low H_2 pressures and corroborates Morkel's assignment of H_2 desorption signals at ~160 K to absorbed H.[19] We further observed (for $T\leqslant260$ K) that the H/Pd ratio does not spontaneously decrease upon H_2 evacuation unless the system is heated above the H_2 exposure temperature at which H was absorbed. The possibility to observe cluster-absorbed H by TPD is hence due to its kinetic inhibition to attain thermal equilibrium with gas phase H_2 in isothermal conditions.

The main advantage of our depth-resolved detection is that H absorbed inside the Pd clusters can be independently probed from H on their surfaces by adjusting the ^{15}N ion energy to a value where the Gaussian surface H signal has decayed to the background, e.g., E_i=6.399 MeV (arrow in Fig. 1). This surface and absorbed H separation is not entirely perfect as, at the large incidence angle, some (~18%) of the ^{15}N ions intersect the Pd clusters and reemerge on the opposite side terrace, where they can detect adsorbed H and may further impinge on a second cluster. This causes surface H signal at $E_i>E_{res}$ due to energy loss of the ^{15}N projectiles inside the intersected cluster. Based on a simulation of randomly arranged crystallites with a minimum separation (10 nm) and area density (~7.5×10^{11} cm^{-2}) as in their STM characterization,[4,5] we determined the impact probability of intersecting ^{15}N ions on a second cluster (~60%) from their spatial pair distribution function. Accounting also for the different incidence angles on the side terraces of the intersected and neighboring Pd clusters, the

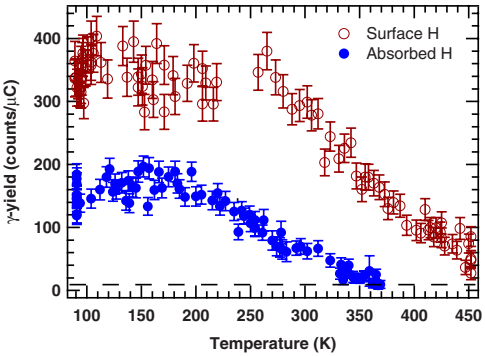

FIG. 2. (Color online) Temperature dependent NRA signals of surface (E=6.385 MeV, 1.5×10^{-3} Pa H_2) and absorbed H (E=6.399 MeV, 9×10^{-5} Pa H_2) in alumina-supported Pd crystallites. The dashed line indicates the small background (10 counts/μC) at E=6.399 MeV due to energy-shifted surface H signal.

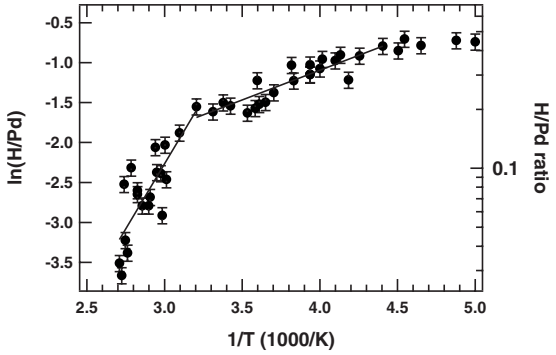

FIG. 3. Arrhenius analysis of the H/Pd ratio in 5.85 Pd/Al_2O_3/NiAl(110) between 200 and 360 K at a H_2 pressure of 9×10^{-5} Pa.

total energy-shifted surface H signal is estimated to be less than 10% of the Gaussian peak intensity at E_{res} that results from direct ^{15}N surface impact. The stopping length variation of the intersecting ^{15}N ions between zero and $z_{max}=h/\cos(\alpha_i)$ (h is the cluster height) further uniformly distributes this intensity over the entire energy range of the depth profile. Thus, the energy-shifted surface H signal at the fixed detection energy of absorbed H (cf. Fig. 2) is negligible at all but the smallest H/Pd ratios (<0.03) and hence not shown in Fig. 1.

The thermal stability of cluster-absorbed H was evaluated by measuring its NRA signal (at E=6.399 MeV) under constant H_2 pressure (9×10^{-5} Pa) as a function of temperature (Fig. 2). The absorbed H quantity is constant below 200 K and decays to the background between 200 and 350 K. Data for surface-adsorbed H measured at $E=E_{res}$ evidence the higher thermal stability of surface H by its decay between 270 and 450 K. Since at $E=E_{res}$ the NRA signal contains significant contribution from absorbed H (cf. Fig. 1), an analysis of these data in terms of the surface adsorption energy is not reasonable. It is instructive, however, to compare Fig. 2 to TPD spectra of Pd/Al_2O_3/NiAl(110) (Fig. 6 of Ref. 20). Here, second-order H_2 desorption between 270 and 400 K (β_2) was assigned to surface-adsorbed H, whereas signals between 200 and 300 K (β_0,β_1) were attributed to absorbed "subsurface" H, yet without further corroboration. The close agreement of these TPD features with the temperature ranges of the thermal decay curves of (mainly) surface and absorbed H NRA signals (Fig. 2) strongly supports the peak assignments of Shaikhutdinov *et al.*[20] Since the β_0 and β_1 H species are associated with a particular reactivity of the Pd nanocrystallites for olefin hydrogenations,[2,3,19,20] our results thus further arguments that absorbed H in the oxide-supported Pd clusters is an important factor for their catalytic activity.

Finally, the data in Fig. 2 are analyzed to evaluate the enthalpy of H solution in the Pd nanocrystals according to

$$\ln(\mathrm{H/Pd}) = \frac{1}{2}\ln\left(\frac{p_{H_2}}{p_0}\right) + \frac{\Delta S_S}{k_B} - \frac{\Delta H_S}{k_B T}, \qquad (2)$$

where the absorbed H signal plateau below 200 K (160 counts/μC) is converted into a H/Pd ratio of 0.52 ± 0.05 by interpolating the H/Pd pressure dependence for 9×10^{-5} Pa. As seen in Fig. 3, the slope of the ln(H/Pd) vs $1/T$ plot continuously varies, reflecting the H/Pd-dependent ΔH_S change due to variations of strain in the expanding Pd lattice and H-H interactions. In the higher ($0.21<\mathrm{H/Pd}<0.45$, $312\ \mathrm{K}>T>227\ \mathrm{K}$) and lower ($0.03<\mathrm{H/Pd}<0.21$, $350\ \mathrm{K}>T>312\ \mathrm{K}$) H concentration regions, the dependence is approximately linear, corresponding to ΔH_S values of $-(0.06\pm0.01)$ eV/H and $-(0.28\pm0.02)$ eV/H, respectively. In the higher H/Pd regime, ΔH_S again fairly agrees with the value for bulk Pd. Whether or not there is a kink at the crossover of the two regimes (H/Pd=0.21 and 312 K) that might correlate to a transition of the Pd clusters from the α to the β phase of PdH_x is not certain given the data noise. In the low H-concentration regime ($0.03<\mathrm{H/Pd}<0.21$), however, the heat of H solution is significantly larger than in bulk Pd [$-(0.1-0.17$ eV)].[18] This indicates that the small Pd crystallites offer a higher stability for absorbed hydrogen than bulk Pd at $\mathrm{H/Pd}<0.2$.

Our depth-resolved analysis indicates that this strong H binding is clearly not due to H on the surface or in first-layer subsurface sites. Even at the grazing ion incidence, H occupation of first-layer subsurface sites remains undistinguishable from H adsorption on the surface and hence does not contribute significant NRA signal at E=6.399 MeV. The observation of strong H stabilization in the Pd cluster volume contrasts the interpretation of the increased H stability observed also for 2–5 nm sized surfactant-stabilized Pd nanoparticles by the assumption of "additional subsurface sites."[6] The latter study ignored that the α-phase H solubility increased to the size of the nanoparticles, i.e., with decreasing surface-to-volume ratio, which contradicts H stabilization at particular sites near or on the surface. On the contrary, this size-dependent trend in Sachs' data is quite consistent with our direct observation that it is the volume of the small Pd particles, which provides enhanced H stabilization compared

to bulk Pd. Our identification of this effect as an intrinsic volume property of the clusters is further corroborated by a very recent x-ray diffraction study that evidenced significant lattice expansion of Pd nanoparticles upon H absorption.[21]

Since our Pd crystallites contain ~6000 atoms, clearly appear metallic in valence band photoemission, and expose cuboctahedral fcc shapes,[2,5] their increased H solubility is not very likely to be due to electronic structure alterations caused by finite size effects. We propose instead that the effect relates to the mostly free surfaces of the Pd crystallites (as well as of the nanoparticles in Sachs' study) because their lattice expansion upon hydrogen absorption faces no resistance by surrounding material. The latter is the case in the macroscopic bulk of polycrystals, where agglomerated grains in close contact invariably exert severe mutual external pressure during H absorption that is manifested, e.g., as the pulverization of hydride storage alloys after repeated H charge and release cycles. That hindrance of the lattice expansion, e.g., by strong interfacial bonds, suppresses H absorption has been demonstrated by thin epitaxial Nb layers on Al_2O_3 substrates[22] or Nb(110) films rigidly clamped between Cu layers.[23] In comparison, an obstruction of the lattice expansion does apparently not occur in our alumina supported Pd clusters, presumably because the Nb/Al_2O_3 adherence is much stronger than that of Pd/Al_2O_3.[24] Although indirectly, the relatively weak Pd/Al_2O_3 metal-support interaction is also evidenced by the near thermal equilibrium crystallite shape[5] in comparison to 300 K deposits of Pt and Rh on the same substrate[2] and by the defect-controlled cluster nucleation during Pd deposition.[2]

A small quantity ($H/Pd < 0.2$) of strongly stabilized H in the Pd crystallites might alternatively be explained by H bonding to the Pd/Al_2O_3 interface, although this appears unlikely as H does not adsorb on the oxide support. Further, in case of significant H accumulation at the interface, predominant intensity is expected in the depth profile of Fig. 1(a) (2×10^{-5} Pa, $H/Pd=0.4$) in the range between $z_{max}=h/\cos(\alpha_i)\approx 8$ nm and $\sim z_{max}/2$, into which the stopping length variation of ^{15}N ions inside the clusters distributes the apparent interface position. However, the "center" of the absorbed H distribution in Fig. 1(a) is located at considerably shallower depth ($\sim z_{max}/4$), which is more consistent with a homogeneous H distribution, giving rise to a NRA depth profile with maximum intensity near the surface that monotonically decreases toward z_{max}, similar to the experimental profile shapes.

In summary, we have collected compelling evidence that the strong α-phase H stabilization in the Pd nanocrystals reflects a volume property of the small particles. Our depth-resolved study has thus revealed that concepts to describe H absorption in isolated nanoparticulates as opposed to macroscopic bulk matter should account for boundary effects on their elastic properties. Such concepts may aid the development of H storage materials and further our understanding of catalysis.

*Corresponding author; wilde@iis.u-tokyo.ac.jp

[1] G. C. Bond, *Metal-Catalyzed Reactions of Hydrocarbons* (Springer, New York, 2005).
[2] M. Bäumer and H.-J. Freund, Prog. Surf. Sci. **61**, 127 (1999).
[3] A. M. Doyle, S. K. Shaikhutdinov, and H.-J. Freund, J. Catal. **223**, 444 (2004).
[4] A. M. Dolye, S. K. Shaikhutdinov, S. D. Jackson, and H.-J. Freund, Angew. Chem., Int. Ed. **42**, 5240 (2003).
[5] K. Hojrup Hansen, T. Worren, S. Stempel, E. Lægsgaard, M. Bäumer, H.-J. Freund, F. Besenbacher, and I. Stensgaard, Phys. Rev. Lett. **83**, 4120 (1999).
[6] C. Sachs, A. Pundt, R. Kirchheim, M. Winter, M. T. Reetz, and D. Fritsch, Phys. Rev. B **64**, 075408 (2001).
[7] S. Kishore, J. A. Nelson, J. H. Adair, and P. C. Eklund, J. Alloys Compd. **389**, 234 (2005).
[8] K. M. Horn and W. A. Lanford, Nucl. Instrum. Methods Phys. Res. B **29**, 609 (1988).
[9] M. Wilde, M. Matsumoto, K. Fukutani, and T. Aruga, Surf. Sci. **482-485**, 346 (2001).
[10] K. Fukutani, M. Wilde, and M. Matsumoto, Phys. Rev. B **64**, 245411 (2001).
[11] M. Wilde and K. Fukutani, Jpn. J. Appl. Phys., Part 1 **42**, 4650 (2003).
[12] J. F. Ziegler, *Handbook of Stopping Cross-Sections for Energetic Ions in All Elements* (Pergamon, New York, 1980).
[13] R. M. Jaeger, H. Kuhlenbeck, H.-J. Freund, M. Wuttig, W. Hoffmann, R. Franchy, and H. Ibach, Surf. Sci. **259**, 235 (1991).
[14] K. Fukutani, A. Itoh, M. Wilde, and M. Matsumoto, Phys. Rev. Lett. **88**, 116101 (2002).
[15] G. E. Gdowski, T. E. Felter, and R. H. Stulen, Surf. Sci. **181**, L147 (1987).
[16] R. J. Behm, K. Christmann, and G. Ertl, Surf. Sci. **99**, 320 (1980).
[17] J. W. Davenport, G. J. Dienes, and R. A. Johnson, Phys. Rev. B **25**, 2165 (1982).
[18] Y. Fukai, *The Metal-Hydrogen System* (Springer, Berlin, 2005).
[19] M. Morkel, M. Rupprechter, and H.-J. Freund, Surf. Sci. **588**, L209 (2005).
[20] S. Shaikhutdinov, M. Heemeier, M. Bäumer, T. Lear, D. Lennon, R. J. Oldman, S. D. Jackson, and H.-J. Freund, J. Catal. **200**, 330 (2001).
[21] H. Kobayashi, M. Yamauchi, H. Kitagawa, Y. Kubota, K. Kato, and M. Takata, J. Am. Chem. Soc. **130**, 1828 (2008).
[22] J. Steiger, S. Blässer, and A. Weidinger, Phys. Rev. B **49**, 5570 (1994).
[23] S. Yamamoto and H. Naramoto, Nucl. Instrum. Methods Phys. Res. B **161-163**, 605 (2000).
[24] A. Bogicevic and D. R. Jennison, Phys. Rev. Lett. **82**, 4050 (1999).